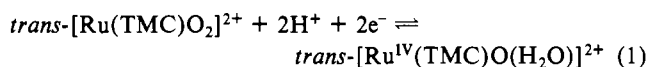
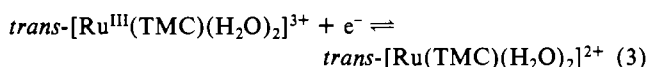
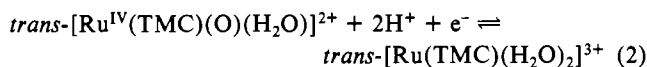


$n$  is the electrochemical stoichiometry. This result, together with the 30–40-mV peak-to-peak separation ( $\Delta E_p$ ) of this couple, strongly suggests that it is a reversible single-step two-electron-transfer process, as represented by eq 1. This is further supported



by the linear plot of  $E_f^\circ$  vs. pH with a slope of 60 mV over the pH range 1–3 (Figure 5) as required by the equation  $E_{298}^\circ = E_f^\circ + 0.059\text{pH}$ .

In acid solutions couples II and III could be assigned to reactions 2 and 3, respectively.



Controlled-potential coulometry of  $\text{trans-}[\text{Ru}^{\text{IV}}(\text{TMC})\text{O}(\text{H}_2\text{O})]^{2+}$  in  $\text{HClO}_4$  (0.1 M) at 0.25 V vs. SCE established  $n = 1$  for reaction 2.<sup>9</sup> All three couples were shifted cathodically, with the two one-electron waves broadening substantially on increasing the pH of the medium. We have also found that Ru(VI) dioxo complexes are particularly unstable at high pH. The  $E_f^\circ$  value for the  $\text{trans-}[\text{Ru}(\text{TMC})(\text{H}_2\text{O})_2]^{3+/2+}$  couple is  $\sim 300$  mV more anodic than that for the corresponding  $\text{trans-}[\text{Ru}(\text{NH}_3)_4(\text{H}_2\text{O})_2]^{3+/2+}$  couple.<sup>10</sup> It is quite likely that this is due to the effect of the TMC ligand as the same difference in  $E_f^\circ$  values has also been found for  $\text{trans-}[\text{Ru}(\text{TMC})\text{Cl}_2]^+$  and  $\text{trans-}[\text{Ru}(\text{NH}_3)_4\text{Cl}_2]^+$ .<sup>7</sup> Whereas  $\text{trans-}[\text{Ru}(\text{NH}_3)_4\text{O}_2]^{2+}$  undergoes complicated chemical reactions upon reduction,<sup>11</sup> the redox inter-

conversion between  $\text{trans-}[\text{Ru}(\text{TMC})\text{O}_2]^{2+}$  and  $\text{trans-}[\text{Ru}(\text{TMC})(\text{H}_2\text{O})_2]^{2+}$  is entirely reversible in strong acids. The cyclic voltammogram of  $\text{trans-}[\text{Ru}(\text{TMC})\text{O}_2]^{2+}$  remains relatively unchanged upon repetitive scanning. The inherent stability of  $\text{trans-}[\text{Ru}^{\text{IV}}(\text{TMC})\text{O}(\text{H}_2\text{O})]^{2+}$  as compared with the analogous  $[\text{Ru}^{\text{IV}}(\text{NH}_3)_4\text{O}(\text{H}_2\text{O})]^{2+}$  (if it does exist) is probably attributed to the macrocyclic as well as the tertiary amine nature of the TMC ligand. Both  $\text{trans-}[\text{Ru}^{\text{IV}}(\text{TMC})\text{O}(\text{H}_2\text{O})]^{2+}$  and  $\text{trans-}[\text{Ru}(\text{TMC})(\text{H}_2\text{O})_2]^{3+}$  could be generated by controlled-potential coulometry. The UV-vis absorption spectrum of the latter cation is shown in Figure 6. Recent kinetic work showed that the chloride anation of  $\text{trans-}[\text{Ru}(\text{TMC})(\text{H}_2\text{O})_2]^{3+}$ , freshly generated electrochemically from  $\text{trans-}[\text{Ru}(\text{TMC})\text{O}_2]^{2+}$ , is just the reverse of the chloride aquation of  $\text{trans-}[\text{Ru}(\text{TMC})\text{Cl}_2]^+$ .<sup>7</sup> This indicates that both  $\text{trans-}[\text{Ru}(\text{TMC})\text{O}_2]^{2+}$  and  $\text{trans-}[\text{Ru}(\text{TMC})\text{Cl}_2]^+$  may have the same geometrical configuration and ligand conformation.

### Conclusion

We have shown here unambiguously the existence of a stable trans Ru(VI) dioxo tetraamine complex. The stability of  $\text{trans-}[\text{Ru}(\text{TMC})\text{O}_2]^{2+}$  and  $\text{trans-}[\text{Ru}(\text{TMC})\text{O}(\text{H}_2\text{O})]^{2+}$  indicates the possibility of developing long-lived oxidative catalysts with high-valent ruthenium macrocyclic amine oxo species.

**Acknowledgment.** We thank the Committee on Research and Conference Grants, University of Hong Kong, for support.

**Registry No.**  $\text{trans-}[\text{Ru}(\text{TMC})\text{O}_2](\text{ClO}_4)_2$ , 95978-18-0;  $\text{trans-}[\text{Ru}(\text{TMC})\text{O}_2](\text{PF}_6)_2$ , 95978-19-1;  $\text{trans-}[\text{Ru}(\text{TMC})\text{Cl}_2]\text{Cl}$ , 92141-42-9;  $\text{trans-}[\text{Ru}(\text{NH}_3)_4\text{O}_2]\text{Cl}_2$ , 38882-90-5;  $\text{trans-}[\text{Ru}(\text{TMC})\text{O}(\text{OH}_2)]^{2+}$ , 92141-47-4;  $\text{trans-}[\text{Ru}(\text{TMC})(\text{H}_2\text{O})_2]^{3+}$ , 95978-20-4;  $\text{trans-}[\text{Ru}(\text{TMC})(\text{H}_2\text{O})_2]^{2+}$ , 95978-21-5.

- (11) Preliminary experiments showed that the reduction of  $\text{trans-}[\text{Ru}(\text{NH}_3)_4\text{O}_2]^{2+}$  or the  $\text{H}_2\text{O}_2$  oxidation of  $\text{trans-}[\text{Ru}(\text{NH}_3)_4(\text{H}_2\text{O})_2]^{3+}$  yielded some ill-defined  $\mu$ -oxo ruthenium amine species: Che, C.M., unpublished results.

(10) Poon, C. K.; Kwong, S. S.; Che, C. M.; Kan, Y. P. *J. Chem. Soc., Dalton Trans.* 1982, 1457-1463.

Contribution No. 3539 from the Central Research & Development Department, Experimental Station, E. I. du Pont de Nemours and Company, Wilmington, Delaware 19898

## Shape Selectivity in Olefin Hydrogenation Using Rhodium-Containing Zeolites

D. R. CORBIN,\* W. C. SEIDEL, L. ABRAMS, N. HERRON, G. D. STUCKY, and C. A. TOLMAN

Received August 8, 1984

Competitive hydrogenation of two cyclic olefins using rhodium zeolite catalysts shows a selectivity based on the molecular dimensions of these substrates. A maximum selectivity of 47 (based on the ratio of hydrogenation rates) is achieved with the medium-pore zeolite ZSM-11 for the preferential hydrogenation of cyclopentene in competition with 4-methylcyclohexene. This selectivity appears to be a composite of the intrinsic size selectivity of the zeolite framework as modified by the presence of intracrystalline water. Rh-X shows selectivities ranging from 1 to 30 as the water content rises while Rh-ZSM-11 displays a maximum in selectivity at an intermediate water content. Selective poisoning of metal sites on the external zeolite surface with bulky phosphines is essential in order to obtain selectivity.

### Introduction

Zeolites are microporous crystalline solids that have been used for ion exchange, as detergents, as drying agents and in the catalytic cracking of petroleum.<sup>1</sup> Recently, chemists have begun to explore the ability of zeolites to impose shape selectivity upon transition-metal-catalyzed reactions since such selectivity may far exceed that possible in homogeneous systems.<sup>2</sup> In their pioneering study, Huang and Schwartz<sup>3</sup> reported that treatment of Linde

13X zeolite with tris( $\pi$ -allyl)rhodium results in a catalyst with improved selectivity toward hydrogenation of small olefins. However, this selectivity was deduced via a comparison of rates for hydrogenation of individual olefins, while to demonstrate true reaction selectivity, one would prefer to compete the two olefins in a single reaction medium. Schwartz also showed that treatment of this catalyst with  $\text{P}(\text{Bu})_3$ , which can only react with surface Rh sites, has little effect on rate, while  $\text{P}(\text{Me})_3$ , which can enter the zeolite, stops catalytic activity.

We have now prepared other rhodium-containing zeolites for comparison with Schwartz's catalyst. In the competitive hydrogenation of cyclopentene and 3- or 4-methylcyclohexene, we observe selectivity increases over that measured for Schwartz's catalyst of an order of magnitude, from 4 to 47. In this paper, we describe the preparation of zeolite catalysts made either by

- (1) Schwachow, F.; Puppe, L. *Angew. Chem., Int. Ed. Engl.* 1974, 14, 620.  
 (2) Dessau, R. M. *J. Catal.* 1982, 77, 304. Chen, N. Y.; Weisz, P. B. *Chem. Eng. Prog., Symp. Ser.* 1967, 63 (No. 73), 86.  
 (3) (a) Huang, T.-N.; Schwartz, J. *J. Am. Chem. Soc.* 1982, 104, 5245. (b) Huang, T.-N.; Schwartz, J.; Kitajima, N. *J. Mol. Catal.* 1984, 22, 389-93.

Table I. Selectivity and Characterization of Rh Zeolites

Rh zeolite	(A) approx channel dimens, Å	(B) selec (sorption) <sup>a</sup>	(C) max selec (reactn) <sup>b</sup>	(D) bulk Rh/Si <sup>c</sup>	(E) surf Rh/Si <sup>d</sup>	(F) surf/bulk <sup>e</sup>	(G) water cont, <sup>f</sup> % by wt
X	7.4	0.91	6.0	0.000 47	<0.003	<6.4	5.0
Y	7.4	0.96	1.0	0.022 00	0.710	35.5	3.6
mordenite	6.7 × 7.0	0.91	16.0	0.015 00	0.093	6.2	8.2
ZSM-34	3.6 × 5.2	0.77	7.5	0.006 10	<0.01	<1.7	
ZSM-11	5.1 × 5.5	1.10	47.0	0.003 20	<0.010	<3.3	2.2
ZSM-5	5.4 × 5.6	1.54	15.0	0.003 30	0.100	33.3	1.2
X ( $\pi$ -allyl)	7.4	0.90	4.0	0.028 90	0.08	2.8	

<sup>a</sup>Selectivity of the anhydrous zeolite (dried at 425 °C in vacuo) for cyclopentane relative to cyclohexane under static conditions by gravimetry.

<sup>b</sup>Observed selectivity of the partially hydrated (see column G) zeolite during the competitive hydrogenation of cyclopentane/4-methylcyclohexane in mixtures. Selectivity quoted is the ratio of hydrogenation rates for the two substrates at their maximum difference. <sup>c</sup>The atomic ratio of rhodium to silicon as determined by zeolite digestion and atomic absorption. <sup>d</sup>The atomic ratio of rhodium to silicon at the zeolite particle surface as probed by XPS. <sup>e</sup>Ratio column E/column D. <sup>f</sup>The residual water content of the zeolites used for hydrogenation that gave rise to the selectivities.

the method of Schwartz (treating with tris( $\pi$ -allyl)rhodium) or by ion exchange. The catalytic selectivity of these catalysts will be discussed on the basis of data from XPS, chemical analysis, and sorption measurements.

We have found that high selectivities depend upon poisoning unselective surface Rh sites, which otherwise dominate the reaction product distribution. Furthermore, while the zeolite support may impart some shape selectivity to the product distribution, we have found that sorbed water in the zeolite framework is also a major factor in determining selectivity.

### Experimental Section

**Synthesis of Triallylrhodium.** This material was prepared as previously described.<sup>4</sup> Diallylrhodium chloride was added in portions to a mixture of 9 cm<sup>3</sup> of allylmagnesium chloride (2 M in THF, Aldrich) and 36 cm<sup>3</sup> of diethyl ether. After the mixture was stirred for 1 h, the flask was stoppered with a rubber septum and removed from the drybox. A thermocouple and small, nitrogen-blanketed vent needle were inserted through the septum, and the solution was cooled to -40 °C. This temperature was maintained during slow addition of the first 5 cm<sup>3</sup> of a total of 60 cm<sup>3</sup> of distilled water. When the water addition was complete, the ether layer was separated and the water layer extracted with a further 30 cm<sup>3</sup> of diethyl ether. The ether layers were combined and dried over anhydrous magnesium sulfate. The crude rhodium complex was recovered by evaporation of the ether. Sublimation at 40 °C (10<sup>-2</sup> torr) yielded 0.6 g of yellow, moderately air-stable, crystals; mp 76–84 °C; lit.<sup>4</sup> mp 80–85 °C. anal. Calcd for C<sub>9</sub>H<sub>15</sub>Rh: C, 47.8; H, 6.6; Cl, 0.0. Found: C, 48.07; H, 6.7; Cl, 0.07.

**Preparation of H<sub>2</sub>Na-X.** A 25-g portion of Na-X (Linde 13X) was slurried in 250 cm<sup>3</sup> of 0.6% ammonium nitrate solution for 3 h at room temperature. After filtering, washing, and drying at 110 °C, the zeolite was calcined in flowing air at 50 °C/h to 540 °C. After it was heated at 540 °C for 10 h, chemical analysis gave a Na/Al ratio of 0.92, indicating approximately 8% H<sup>+</sup> exchange. No significant loss in crystallinity was observed in the X-ray powder pattern of the calcined product.

**Reaction of Triallylrhodium with 8% H<sub>2</sub>Na-X Zeolite.** A 1.6-g sample 8% H<sub>2</sub>Na-X zeolite from above was slurried in 19 cm<sup>3</sup> of *n*-octane. A solution of 0.085 g of triallylrhodium in 5 cm<sup>3</sup> of *n*-octane was added dropwise to the well-stirred zeolite slurry at room temp. The yellow color of the solution transferred rapidly to the zeolite, and the reaction mixture was allowed to stand for 60 h. The zeolite was then filtered, vacuum dried, and used for selective hydrogenation experiments without further treatment.

**Preparation of Rhodium-Exchanged Zeolites. Zeolite X.** A 10-g sample of Na-X (Linde 13X) was slurried in 500 cm<sup>3</sup> of 1.0 mM RhCl<sub>3</sub>. After 24 h at 90 °C, the zeolite was filtered, washed, and dried at 110 °C. Chemical analysis indicates 0.031% Rh, which corresponds to 0.05 rhodium ions per unit cell.

**Zeolite Y.** A 20-g sample of Na-Y (Linde LZ-Y52) was slurried in 500 cm<sup>3</sup> of 8.1 mM RhCl<sub>3</sub>. After 16 h at 90 °C, the zeolite was filtered, washed with distilled water, and dried at 110 °C. Chemical analysis indicates 1.98% Rh or 3.1 rhodium ions per unit cell.

**Mordenite.** A 20-g sample of Na-mordenite (Linde M-5) was slurried in 500 cm<sup>3</sup> of 8.1 mM RhCl<sub>3</sub>. After 16 h at 90 °C, the zeolite was filtered, washed with distilled water, and dried at 110 °C. Chemical analysis indicates 1.90% Rh or 0.6 rhodium ion per unit cell.

**ZSM-34.** Na,K-ZSM-34 was prepared by literature methods<sup>5</sup> and calcined in flowing air at 50 °C/h to 540 °C and then held at 540 °C for 10 h to remove the choline chloride template. A 20-g portion was then slurried in 500 cm<sup>3</sup> of 2.9 mM RhCl<sub>3</sub> at 90 °C for 16 h. After filtering and washing, the sample was dried at 110 °C. Chemical analysis indicates 0.72% Rh or 0.25 rhodium ion per unit cell.

**ZSM-11.** Na-ZSM-11 was prepared by a modification of the literature method.<sup>6</sup> NaAlO<sub>2</sub> (1.8 g) and NaOH (2.4 g) in water (92 g) were added to a second solution containing Ludox HS-30 silica sol (120 g), tetrabutylammonium bromide (19.34 g), and water (40 g). The resulting gel was stirred under autogeneous pressure at 160 °C for 24 h, and the solid produced was thoroughly washed and dried at 110 °C. The X-ray powder diffraction pattern corresponded to that of Na,TBA-ZSM-11.<sup>7</sup> The zeolite was calcined in flowing air at 50 °C/h to 540 °C and then held at 540 °C for 10 h. Si/Al ratio was 32. A 10-g portion was then slurried in 500 cm<sup>3</sup> of 1.0 mM RhCl<sub>3</sub> at 90 °C for 16 h. After filtering, washing, and drying at 110 °C, chemical analysis indicates 0.49% Rh or 0.3 rhodium ion per unit cell.

**ZSM-5.** Na,TPA-ZSM-5 (Si/Al ratio 41) was prepared by literature methods<sup>8</sup> and calcined in flowing air at 60 °C/h to 550 °C and then held at 550 °C for 10 h. A 10-g portion was slurried in 500 cm<sup>3</sup> of 1.0 mM RhCl<sub>3</sub> at 90 °C for 24 h. After filtering, washing, and drying at 110 °C, chemical analysis shows 0.48% Rh or 0.31 rhodium ion per unit cell.

The above exchange procedures are modifications of those used by Shannon et al.<sup>8</sup> to produce well-characterized rhodium in zeolite species.

**Sorption Characterization of Zeolites.** A sample of zeolite was heated to 425 °C under vacuum in a preweighed cell employing a leak-tight vacuum stopcock. It was then pumped to a residual pressure of  $\sim 2 \times 10^{-5}$  mm, cooled, and weighed. Subtraction of the evacuated cell weight provides the weight of the dry, evacuated zeolite as well as its initial water content.

The cell was then attached to an adsorption manifold where the zeolite was exposed to the solvent vapor for 20 h at room temperature. Subtracting the cell and evacuated zeolite weights provided the weight sorbed by the zeolite in each cell. The amount sorbed per gram was calculated and used as a basis of comparison to generate Table I (column B).

**Hydration State of Zeolites.** The water contents of the above zeolites as used for hydrogenation experiments were measured by weight loss at 425 °C under vacuum as described above. Samples of Rh-X and Rh-ZSM-11 were allowed to stand over a saturated ammonium nitrate solution in a closed desiccator for  $\sim 60$  h in order to fully hydrate prior to the hydrogenation runs. Further portions of these same two zeolites were dehydrated at 125 °C under 10<sup>-4</sup> torr vacuum for 36 h before additional hydrogenation runs in order to estimate the relative effects of water content and pore size on selectivities. Samples of Rh-ZSM-11 with intermediate levels of hydration were prepared by successively adding weighed quantities of water to a weighed portion of the dehydrated zeolite followed by equilibration at room temperature for 24 h in a sealed vessel prior to the hydrogenation run.

**Olefin Hydrogenations.** All operations were conducted in a Vacuum Atmospheres drybox under dry nitrogen. Olefins and product alkanes were analyzed on either a 10- or 20-m methyl silicone capillary GC column in either a Hewlett-Packard 5880 or a Perkin-Elmer 3920B gas chromatograph. A temperature program from 40 to 80 °C at 4°/min

(5) Ruben, M. K.; Rosinshi, E. J.; Plant, C. J. U.S. Patent 4 086 186, 1978.

(6) Rollman, L. S.; Volyosick, E. W. *Inorg. Synth.* 1983, 22, 61–68.

(7) Argauer, R. J.; Landolt, G. R. U.S. Patent 3 702 886, 1972. Chu, P. U.S. Patent 3 709 979, 1973.

(8) Shannon, R. D.; Vadrine, J. C.; Naccache, C.; Lefebvre, F. *J. Catal.* 1984, 88, 431.

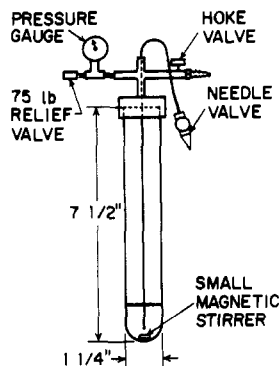


Figure 1. Pressure bottle apparatus used in the hydrogenation reactions.

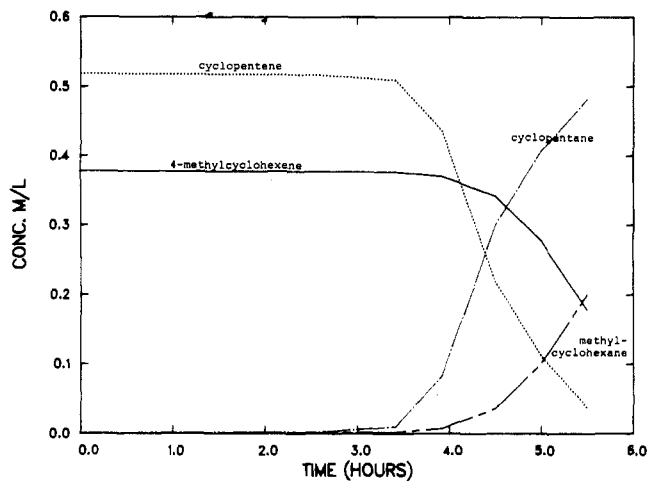


Figure 2. Typical experimental data from a hydrogenation using 58% hydrated Rh-ZSM-11 catalyst. Plot of concentrations of hydrocarbons as a function of time.

resolved all reactants and products. The olefins cyclopentene, 3-methylcyclohexene, and 4-methylcyclohexene (Aldrich) were purified by passage over a 10-cm column of alumina. The reduction products cyclopentane and methylcyclohexane were identified by GC/MS comparison with genuine samples. In a typical experiment, a mixture of 0.030 g of Rh zeolite, 65 cm<sup>3</sup> of *n*-octane, 0.3 cm<sup>3</sup> of cyclopentene, and 0.3 cm<sup>3</sup> of methylcyclohexene were charged to a Fischer-Porter bottle equipped with a dip leg, pressure-relief valve, and magnetic stir bar (Figure 1). A 5- $\mu$ L portion of PBU<sub>3</sub> was added with stirring, and the bottle was closed and pressurized with hydrogen to 50 psi. The fully charged vessel was placed in a magnetically stirred oil bath at 60 °C, and samples were taken periodically by opening the dip leg valve and withdrawing a small portion. A typical result is shown in Figure 2. Selectivities in hydrogenation reactions were estimated as the ratio of the rates of reactant olefin consumption or product alkane appearance at the maximum rate of reaction. All reactions using Rh(III) zeolites exhibited a variable induction period of from 1 to 20 h before reaction began. This time probably represents that needed for reduction of the ions to Rh(0) since prereduction with hydrogen eliminated the phenomenon. This induction period appears to be essentially independent of the residual water content of the zeolite.

### Results and Discussion

All of the zeolites chosen for this study have pore dimensions large enough so that at least one of the reactant olefins should be able to gain access to the intracrystalline voids. This is confirmed by sorption measurements with cyclopentane (with molecular dimensions of 3.5  $\times$  5.4 Å) and cyclohexane (5.0  $\times$  5.8 Å) (these being chosen as probe molecules because of their similar molecular dimensions to the reactant olefins). These sorption measurements, performed on the dehydrated (425 °C, vacuum) zeolites, also indicate the intrinsic size selectivity of the zeolite framework itself (column B of Table I). The selectivities of the various catalysts for hydrogenation of the two olefins are listed in Table IC. In almost all instances, the observed hydrogenation selectivities are superior to that observed with Schwartz's zeolite catalyst (selectivity  $\approx$  4).<sup>9</sup> It is clear, however, that there is no

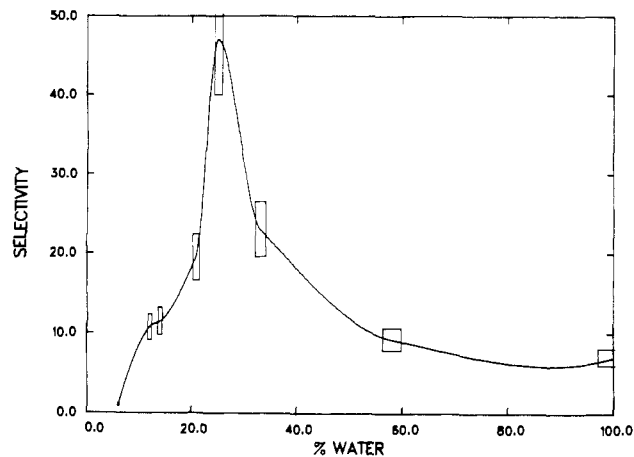


Figure 3. Selectivity in hydrogenation of cyclopentene/4-methylcyclohexene mixtures as a function of hydration level of the catalyst Rh-ZSM-11. The x axis is expressed in terms of percent of the total possible water capacity i.e., 100% on this scale  $\approx$  8.8% water by weight.

direct correlation between the selectivity predicted by sorption measurements and the observed reaction selectivity. For example, sorption data predicts that Rh-ZSM-5 should be the most selective catalyst rather than Rh-ZSM-11. This observation may be explained by the concept of "molecular traffic control".<sup>10</sup>

Clearly, factors other than simple pore size differences control the observed reaction selectivities. One such factor, metal siting, was suspected of being important and in Table I (columns D-F) is a comparison of the bulk Rh/Si ratio (atomic absorption) to that of the surface layers (XPS). Metal sites on the external surface of the zeolite would be expected to be relatively non-size-selective and, because of their accessibility, might be expected to dominate the product distribution. These external sites can be selectively poisoned, however, by using the same approach adopted by Schwartz:<sup>3a</sup> i.e., treating the zeolites with the bulky PBU<sub>3</sub>. This ligand is too large to access the internal metal sites, and indeed such treatment leads to a dramatic increase in selectivity, e.g., a factor of 4 for Rh-ZSM-11. Treatment with a small phosphine (PMe<sub>3</sub>) kills all activity. All of the catalysts listed in Table I were therefore treated with PBU<sub>3</sub> to maximize selectivity; however, those results still indicate that a further major factor contributing to reaction selectivity is operative.

Such a factor may well be the presence of variable water content (Table I, column G). All of the zeolite catalysts were partially hydrated at the beginning of each hydrogenation run, and the effect of this water was investigated for the Rh-X and Rh-ZSM-11 zeolites. The Rh-X catalyst was run in three hydration states (2%, ~5%, and 32% water by weight) and gave selectivities of 1, 6, and 30, respectively. The dramatic effect on the reaction selectivity can be rationalized as follows. In the absence of water, one observes the intrinsic size selectivity of the zeolite framework which in the case of X zeolite would be expected to be unimportant (Table I, column B). As the moisture content rises, it will tend to line the internal cations, pores, and chambers of the zeolite with a coating of water and thereby effectively reduce the internal pore dimensions. This will, in turn, increase the size selectivity of this zeolite toward the two olefins. Apart from this effect on selectivity, the presence of water also dramatically affects the rate of hydrogenation; it is some 20 times slower for the 32% water content catalyst compared to that with 2%.

The Rh-ZSM-11 catalyst was also run with various degrees of hydration, and in this case a maximum is apparent in the selectivity vs. degree of hydration curve (Figure 3). The selectivity

- (9) This selectivity should be compared with the value of  $\sim$ 25 as inferred from the hydrogenation rates of the individual olefins.<sup>3a</sup> This large discrepancy is apparently the result of performing a truly competitive reaction as opposed to inferring selectivity from individual rate data.
- (10) Derouane, E. G.; Dejaive, P.; Gabelica, Z.; Vadrine, J. *Faraday Discuss. Chem. Soc.* 1981, 72, 331. Derouane, E. G. *J. Catal.* 1981, 72, 177.

at low water content is  $\sim 1$ , in agreement with sorption data (column B, Table I) and at full hydration is only  $\sim 7$ . However, at intermediate levels of hydration the selectivity peaks at  $\sim 47$ . It appears that at this level of hydration the water sheath adhering to the zeolite channels has optimized this dimension for selection between the olefins.<sup>11</sup>

These observations suggest, therefore, that the dichotomy between columns B and C of Table I is best explained in terms of

- (11) An alternative interpretation for this observed effect of water content might consider the water to be modifying the active rhodium sites by coordination. This effect has been shown by Rylander: Rylander, P. L. "Catalytic Hydrogenation over Platinum Metals"; Academic Press: New York, 1967; p 328. While this type of effect may contribute to altered selectivities, we feel that the appearance of a maximum in, and the general shape of, the selectivity curve (Figure 2) is better explained if the proposed mechanism of pore size modification is the major contributor to selectivity. Experiments to clarify this point further will be performed in these laboratories.

the effect of the residual water content of the catalysts (Table I, column G) in modifying the framework size selectivity.<sup>12</sup> This latter observation indicates that a delicate balance exists between selectivities based on pore size and on moisture content. This situation probably occurs in any catalytic system employing a zeolite (particularly when water is a byproduct of the catalytic reaction) and the marked contribution of moisture content toward catalytic selectivity should not be overlooked.

**Acknowledgment.** The authors thank Dr. P. E. Bierstedt for the XPS measurements and J. B. Jensen, G. F. Diffendall, W. B. Arters, and R. W. Shiffer for technical assistance. We also thank Dr. J. Schwartz for helpful discussions and advice on the preparation of the Rh-allyl-X catalyst.

**Registry No.** Rh, 7440-16-6; tris( $\pi$ -allyl)rhodium, 12082-48-3.

- (12) Breck, D. W. "Zeolite Molecular Sieves"; Wiley: New York, 1974; pp 644-45.

Contribution from the Department of Chemistry,  
Washington State University, Pullman, Washington 99164-4630

## Reduction Potential and Bonding Trends in Manganese(I) and Manganese(II) Hexakis(aryl and alkyl isocyanides)

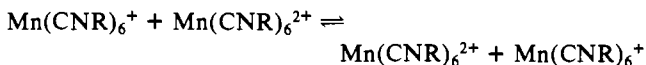
ROGER M. NIELSON and SCOT WHERLAND\*

Received September 7, 1984

This paper presents infrared, Raman, and cyclic voltammetry results on  $\text{Mn}(\text{CNR})_6\text{BF}_4$  and  $\text{Mn}(\text{CNR})_6(\text{BF}_4)_2$  complexes, where R is methyl, ethyl, isopropyl, *tert*-butyl, cyclohexyl, benzyl, phenyl, *p*-tolyl, and *p*-anisyl. These results are interpreted with the aid of self-consistent field *ab initio* calculations (GAUSSIAN 76) on the ligands. The  $E_{1/2}$  values correlate well with the energy calculated for the lowest energy  $\pi^*$  orbital of the ligands. It is concluded that the  $E_{1/2}$  values reflect the HOMO energy of the complexes. The back-bonding is further probed by using the observed trends in the apparent MnC and CN force constants. It is concluded that the CN force constants and vibrational frequencies are not good measures of the back-bonding interaction when alkyl and aryl isocyanide complexes are being compared because of the delocalized nature of the HOMO in the aromatic case.

### Introduction

We became interested in manganese isocyanide complexes because of their electron-transfer reactivity. We have previously investigated the effect of solvent and added salt on the electron self-exchange reaction



in which R is cyclohexyl,<sup>1</sup> and in acetonitrile only we have investigated the effect of varying the R group over the range methyl, ethyl, isopropyl, *tert*-butyl, and benzyl.<sup>2</sup> The first study generally showed a lack of correlation with the solvent dielectric continuum theory of solvent reorganization and established the effect of ion pairing as distinct from the effect of ionic strength. The second study demonstrated a decrease in electron-transfer rate constant with increasing ligand bulk. This is the best example of such an effect in bimolecular chemistry. The benzyl isocyanide complex exhibited a somewhat higher reactivity than would be predicted from its size. Studies currently in progress on phenyl, *p*-tolyl, and *p*-anisyl isocyanide complexes demonstrate a greatly enhanced reactivity compared to alkyl ligands of similar size. The most obvious interpretation of the enhanced reactivity for the phenyl series, and possibly the benzyl compound, is that  $\pi$  bonding allows electron density from the manganese nucleus to be delocalized onto the ligand, thus effectively decreasing the electron-transfer distance.

In order to further characterize these compounds and investigate the extent of delocalization, we have made a series of physical measurements. These include <sup>55</sup>Mn, <sup>14</sup>N, <sup>13</sup>C, and <sup>1</sup>H NMR, EPR, room-temperature solution and solid-state magnetic susceptibility, infrared, Raman, ultraviolet spectroscopy, cyclic voltammetry, and several *ab initio* molecular orbital (MO) calculations on the ligands alone.

Some spectroscopic, electrochemical,<sup>3,4</sup> and quantum-mechanical calculation data<sup>5,6</sup> are available in the literature for these complexes. These data are limited to some <sup>1</sup>H<sup>7</sup> and <sup>14</sup>N NMR<sup>8</sup> data, EPR,<sup>7,9</sup> ultraviolet absorption measurements,<sup>6,10</sup> infrared data<sup>11</sup> on most of the complexes, and Raman data for the methyl and phenyl isocyanide complexes.<sup>12</sup> Of these data, we have been unable to reproduce the EPR and <sup>1</sup>H NMR results for the Mn(II) complexes, as discussed elsewhere.<sup>13</sup>

Our results on the physical properties have been divided into two reports. This paper discusses the Raman, infrared, cyclic

(1) Nielson, R. M.; Wherland, S. *Inorg. Chem.* 1984, 23, 1338.

(2) Nielson, R. M.; Wherland, S. *J. Am. Chem. Soc.* 1985, 107, 1505.

(3) Treichel, P. M.; Mueh, H. J. *Inorg. Chem.* 1977, 16, 1167.

(4) Gritzner, G. *Monatsh. Chem.* 1976, 107, 1499.

(5) Sarapu, A. C.; Fenske, R. F. *Inorg. Chem.* 1975, 14, 247.

(6) Fantucci, P. C.; Valenti, V.; Cariati, F. *Inorg. Chim. Acta* 1971, 5, 425.

(7) Fantucci, P. C.; Naldini, L.; Cariati, F.; Valenti, V. *J. Organomet. Chem.* 1974, 64, 109.

(8) Becker, W.; Beck, W.; Rieck, R. Z. *Naturforsch., B: Anorg. Chem., Org. Chem., Biochem., Biophys., Biol.* 1970, 25B, 1332.

(9) Matteson, D. S.; Bailey, R. J. *J. Am. Chem. Soc.* 1969, 91, 1975.

(10) Mann, K. R.; Cimolino, M.; Geoffroy, G. L.; Hammond, G. S.; Orio, A. A.; Albertin, G.; Gray, H. B. *Inorg. Chim. Acta* 1976, 16, 97.

(11) Cotton, F. A.; Zingales, F. J. *J. Am. Chem. Soc.* 1961, 83, 351.

(12) Verdonck, L.; Tulun, T.; Van der Kelen, G. P. *Spectrochim. Acta, Part A* 1979, 35A, 867.

(13) Nielson, R. M.; Wherland, S. *Inorg. Chem.*, in press.